Sensors and Materials, Vol. 30, No. 7 (2018) 1577–1583
MYU Tokyo

S & M 1613

New Intrinsic Scintillator with Large Effective Atomic Number: Tl_2HfCl_6 and Tl_2ZrCl_6 Crystals for X-ray and Gamma-ray Detections

Yutaka Fujimoto,[1*] Keiichiro Saeki,[1] Daisuke Nakauchi,[2]
Takayuki Yanagida,[2] Masanori Koshimizu,[1] and Keisuke Asai[1]

[1]Department of Applied Chemistry, Graduate School of Engineering, Tohoku University,
Sendai, Miyagi 980-8579, Japan
[2]Graduate School of Materials Science, Nara Institute of Science and Technology,
8916-5 Takayama, Ikoma, Nara 630-0192, Japan

(Received January 22, 2018; accepted March 27, 2018)

Keywords: scintillator, crystal growth, Tl_2HfCl_6, Tl_2ZrCl_6

We report on the photoluminescence and scintillation characterizations of new Tl_2HfCl_6 and Tl_2ZrCl_6 crystalline scintillators grown by the vertical Bridgman–Stockbarger method. Both Tl_2HfCl_6 and Tl_2ZrCl_6 crystals showed an intrinsic emission band peak at 450–470 nm under UV light and X-ray excitations. The scintillation light yields of Tl_2HfCl_6 and Tl_2ZrCl_6 reach 24200 and 50800 photons/MeV, respectively. Their energy resolutions at 662 keV are 17.7% for Tl_2HfCl_6 and 5.6% for Tl_2ZrCl_6. The scintillation decay time values of Tl_2HfCl_6 are 288 and 6340 ns; meanwhile, those of Tl_2ZrCl_6 are 696 and 2360 ns.

1. Introduction

Inorganic crystalline scintillators have been in use for decades to detect and measure X-ray and gamma-ray radiations as they provide an efficient means of converting a high-energy electromagnetic radiation into ultraviolet-visible photons of light that can be detected with photosensitive sensors such as a photomultiplier tube (PMT) and a photodiode (PD). The ultraviolet-visible photons are converted into a current pulse signal to be quickly counted and recorded by the PMT and PD, and thus, the scintillator-based radiation detectors belong to the indirect detector category. The number of scintillation photons as a response to a high-energy electromagnetic radiation is proportional to the current signal. Thus, the advancement of the radiation detector's performance cannot be realized without the discovery of new scintillators with superior characteristics and the improvement of the existing scintillators. For X-ray and gamma-ray spectroscopy applications, the scintillator material must possess, in general, a large effective atomic number (Z_{eff}), a high light yield with good energy resolution, and a fast decay time constant. In particular, the large Z_{eff} provides high photoelectric conversion efficiencies of X-rays and gamma-rays [the probability of absorption by the photoelectric effect is proportional

*Corresponding author: e-mail: fuji-you@qpc.che.tohoku.ac.jp
http://dx.doi.org/10.18494/SAM.2018.1927

ISSN 0914-4935

to ρZ_{eff}^{3-4} (ρ, density)].[1] Although a classical NaI:Tl (Z_{eff} = 50.8) scintillator and some currently developed halide scintillators, such as SrI_2:Eu (Z_{eff} = 50.3) and $CeBr_3$ (Z_{eff} = 47.6), have demonstrated a high light yield and good energy resolution,[2–3] their Z_{eff} values are less than those of oxide-based commercial scintillators such as Gd_2SiO_5:Ce (Z_{eff} = 59.4), Lu_2SiO_5:Ce (Z_{eff} = 65.4), and $Bi_4Ge_3O_{12}$ (Z_{eff} = 75.2). Recent studies of a new scintillator material for X-rays and gamma-rays focus on Tl- and Hf-based halide scintillators because of the large atomic numbers of Tl (81) and Hf (72). Burger and co-workers have worked on the development of new Hf-based intrinsic halide scintillators and reported Cs_2HfCl_6 and $Cs_2HfCl_4Br_2$ crystals having high Z_{eff} values, high light yields, and good energy resolution.[4,5] Other research groups studied various Tl-based alkali halide elpasolite scintillators activated with Ce^{3+}.[6–9] Among the elpasolite scintillators, the Tl_2LiYCl_6:Ce (TLYC) crystal shows good scintillation properties. Moreover, the TLYC crystal can distinguish gamma-ray and neutron radiations by pulse shape discrimination (PSD).[9] Presently, our group has also reported some new halide scintillator materials with low hygroscopicity and large Z_{eff} values, namely, $CsPbCl_3$,[10] Cs_3BiCl_6,[11] Rb_2HfCl_6,[12] $TlMgCl_3$,[13] $TlCdCl_3$,[14] and Cs_2HfBr_6.[15] In particular, Rb_2HfCl_6, $TlMgCl_3$, and Cs_2HfBr_6 scintillators were very interesting because they show high light yields and good energy resolution without any internal doping of an emission center. This study focused on two intrinsic halide scintillators containing Tl and Hf ions, namely, Tl_2HfCl_6, and Tl_2ZrCl_6. To the best of our knowledge, no other study on crystal growth, photoluminescence, and scintillation properties of Tl_2HfCl_6 and Tl_2ZrCl_6 has been reported so far. The two crystals have large Z_{eff} values (72.7 for Tl_2HfCl_6 and 70.7 for Tl_2ZrCl_6), resulting in excellent photoelectric conversion efficiencies of X-rays and gamma-rays. We present and discuss results from the initial study of Tl_2HfCl_6 and Tl_2ZrCl_6 crystalline scintillators, grown by the vertical Bridgman–Stockbarger method, in the following sections.

2. Experimental Procedure

Samples of Tl_2HfCl_6 and Tl_2ZrCl_6 crystals were prepared by the vertical Bridgman–Stockbarger method. Mixtures of TlCl (99.9%, Mitsuwa Chemicals Co., Ltd.) and $HfCl_6$ (99.9%, Mitsuwa Chemicals Co., Ltd.) or $ZrCl_6$ (99.99%, Sigma-Aldrich) raw materials in stoichiometric ratio were used for the growth of Tl_2HfCl_6 and Tl_2ZrCl_6 crystals. The mixtures were then loaded into precleaned and prebaked quartz ampoules. The mixtures in the quartz ampoules were dried by heating overnight at 573 K in vacuum for 72 h before sealing. The crystal growth was carried out under vacuum in the sealed quartz ampoule using the vertical Bridgman furnace (TBR-30V, Techno Search Corp.). The ampoule was pulled down at a rate of 1.0–3.0 mm/h from top to bottom in a gradient temperature zone. The temperatures of the upper and lower zones in the vertical furnace were 1273 and 1073 °C, respectively, resulting in the temperature gradient of 1.3 K/mm across the solid-liquid interface. After the crystal growth was finished, the furnace was cooled to room temperature at a speed of 20 °C/h. As-grown crystals (shown in Fig. 1) were cut and polished into dimensions of 2.0 × 1.0 × 1.0 mm^3 for use in photoluminescence and scintillation measurements. The measurements were carried out in air atmosphere because the visual observation indicated that the crystals are less hygroscopic than SrI_2:Eu and $LaBr_3$:Ce crystals.

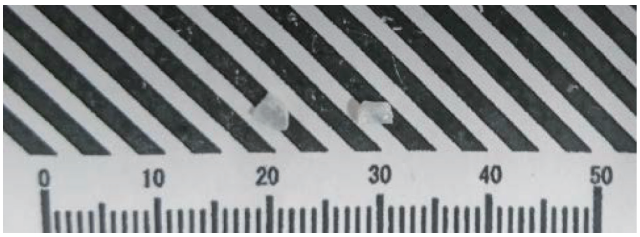

Fig. 1. (Color online) Photograph of as-grown Tl_2HfCl_6 (left) and Tl_2ZrCl_6 (right) crystals.

The photoluminescence spectra were evaluated using an F-7000 (Hitachi High-Technologies) fluorescence spectrophotometer. The photoluminescence decay curves were measured with a DeltaFlex time-correlated single-photon counting system (Horiba). The crystal samples were excited at 250 nm using a pulsed NanoLED excitation source. The obtained decay curves were fitted to the appropriate exponential model after the deconvolution of the instrument response function.

The scintillation spectra were measured by excitation with X-rays from an X-ray generator (RINT2200, Rigaku) equipped with a copper target at power settings of 40 kV and 40 mA. The scintillation photons from the samples were counted with a SILVER-Nova multichannel spectrometer (Stellarnet Inc.) that was cooled to −15 °C using a Peltier module through an optical fiber. The crystal samples were optically coupled to the fiber head using optical grease, and Teflon tape was used as a reflector to enhance the light collection of diffuse reflections.

The scintillation decay time profiles were evaluated using a customized-setup, pulsed X-ray-induced scintillation characterization system (Hamamatsu Photonics).[16] The main modules of the system are an R7400P-06 PMT (Hamamatsu Photonics) and an X-ray tube (N5084, Hamamatsu Photonics) controlled by a picosecond laser diode (PLP10-063, Hamamatsu). By combining the laser diode and X-ray tube, a pulsed X-ray was generated. The PMT was used to count scintillation photons in the photon-counting mode, and the detectable wavelength region of the PMT was 160 to 650 nm.

The scintillation pulse height spectra with 662 keV gamma-rays from a ^{137}Cs souce were evaluated using the sample crystals optically coupled to an R7600-200 PMT (Hamamatsu). The experimental details were described in our previous report.[17] For better light collection, crystal samples were wrapped with Teflon tape on all sides, except the face in contact with the window of the PMT. The PMT was connected to an ORTEC 113 preamplifier, an ORTEC 572 shaping amplifier, and an Amptec 8000A multichannel analyzer (MCA). The spectra were recorded with a 10 μs shaping time. The quantum efficiency (QE) of the PMT was calculated using the wavelength response of the PMT and the scintillation spectra. The scintillation light yield was calculated by comparing the 662 keV gamma-ray-induced photopeak position of the samples with the position of the peak in spectra collected with a NaI:Tl commercial scintillator (*LY* = ~40000 photons/MeV).

3. Results and Discussion

Figures 2(a) and 2(b) illustrate the obtained photoluminescence spectra of Tl_2HfCl_6 and Tl_2ZrCl_6 crystals. The intrinsic emission peak at 450–470 nm was observed upon ultraviolet light excitation for both Tl_2HfCl_6 and Tl_2ZrCl_6 crystals. This indicates that at least the emission process of Tl_2HfCl_6 is similar to that of Tl_2ZrCl_6. When monitoring emission at 465 nm, excitation bands at 255 nm for Tl_2HfCl_6 and at 270 nm for Tl_2ZrCl_6 were observed. Similar excitation bands were reported previously for Cs_2HfCl_6 and Cs_2ZrCl_6 crystals, and they correspond to charge transfer on $HfCl_6^{2-}$ and $ZrCl_6^{2-}$ complex ions. Considering the obtained photoluminescence spectra and referring to some previous studies about luminescence and optical characterizations of Cs_2HfCl_6 and Cs_2ZrCl_6 crystals, the origin of the blue emission band is possibly self-trapped excitons (STEs) that strongly depend on the Zr^{4+} impurity in the host crystal.[18–20] Zr^{4+} was detected as a major contaminant of the hafnium chloride ($HfCl_4$) raw material and grown Hf-containing halide crystals,[4,19,21] resulting in the creation of several types of STE states and the intrinsic luminescence of the Tl_2HfCl_6 crystal, which is similar to that of the Tl_2ZrCl_6 crystal.

The photoluminescence decay curves of Tl_2HfCl_6 and Tl_2ZrCl_6 crystals are shown in Figs. 3(a) and 3(b), respectively. From the exponential fitting calculation, the decay time values of Tl_2HfCl_6 were approximately 324 and 3560 ns, whereas those of Tl_2ZrCl_6 were found to be approximately 360 and 3860 ns. The decay time value of Tl_2HfCl_6 was close to that of Tl_2ZrCl_6 because of the similar origins of the emission.

Figure 4 illustrates the scintillation spectra of Tl_2HfCl_6 and Tl_2ZrCl_6 crystals. The spectrum of Cs_2ZrCl_6 (black dotted line) is also presented for comparison. The spectra of both Tl_2HfCl_6 and Tl_2ZrCl_6 crystals show an emission band peak at 450–470 nm. The spectra are consistent with the photoluminescence spectra, and thus, the peak can be assigned to the STEs. A similar emission band was observed for the Cs_2ZrCl_6 crystal. The slight shift in emission wavelength may be due to the difference in the monovalent cation between Cs^+ and Tl^+ since a similar emission shift was observed previously for Cs_2HfCl_6 and Rb_2HfCl_6.[12]

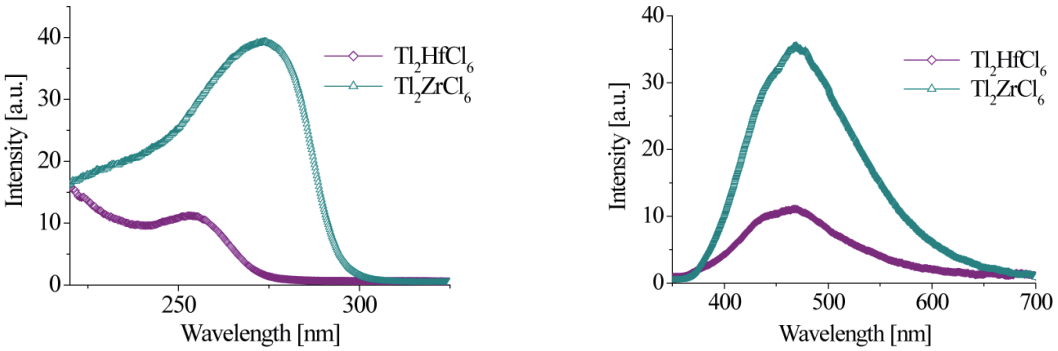

Fig. 2. (Color online) (a) Excitation and (b) emission spectra of Tl_2HfCl_6 and Tl_2ZrCl_6 crystals (λ_{em} = 465 nm; λ_{ex} = 255 nm for Tl_2HfCl_6 and 270 nm for Tl_2ZrCl_6).

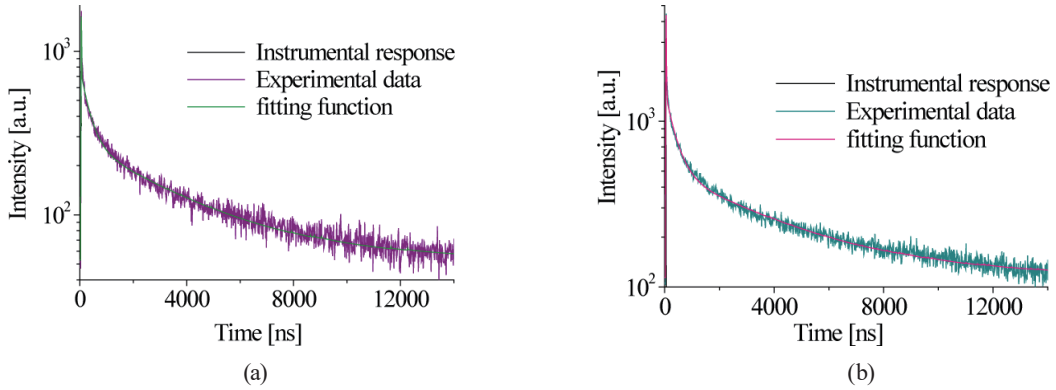

Fig. 3. (Color online) Photoluminescence decay curves of (a) Tl_2HfCl_6 and (b) Tl_2ZrCl_6 crystals (λ_{em} = 465 nm, λ_{ex} = 250 nm).

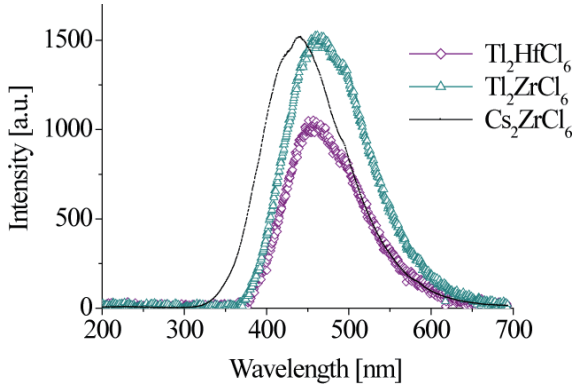

Fig. 4. (Color online) X-ray excited scintillation spectra of Tl_2HfCl_6 (purple squares) and Tl_2ZrCl_6 (green triangles) crystals and a Cs_2ZrCl_6 crystal (black line) for comparison.

The scintillation decay profiles of Tl_2HfCl_6 and Tl_2ZrCl_6 crystals are shown in Figs. 5(a) and 5(b), respectively. The decay time values were calculated to be approximately 288 and 6340 ns for Tl_2HfCl_6 and 696 and 2360 ns for Tl_2ZrCl_6. From the measurements, the decay of Tl_2HfCl_6 and Tl_2ZrCl_6 crystals was found to be faster than that of Cs_2HfCl_6 (2200 and 8400 ns) and Cs_2ZrCl_6 (1500 and 7500 ns) reported previously.[21] This is possibly caused by the difference in STE type between Cs_2MCl_6 and Tl_2MCl_6 (M = Hf, Zr). This difference is dependent on the crystal structure, crystalline quality, and localized electronic state. Understanding the mechanism of the difference in decay time value between photoluminescence and scintillation is clearly beyond the scope of our present study; however, we speculate that it is due to a complex energy transfer process from the host crystal lattice to emission centers under excitation by ionizing radiations.[22]

Figure 6 illustrates the scintillation pulse height spectra of Tl_2HfCl_6 and Tl_2ZrCl_6 crystals, and the NaI:Tl commercial scintillator. In the spectra, the ^{137}Cs-662 keV gamma-ray photopeaks of the Tl_2HfCl_6 and Tl_2ZrCl_6 crystals were located at the 250 and 525 channels, while that of the NaI:Tl commercial scintillator was observed at the 590 channel. Another peak at the 475 channel was also observed for Tl_2ZrCl_6 owing to the escape of K_β and K_α X-rays from Tl atoms of the crystal.[23] The QEs of the R7600U PMT at 465 (Tl_2HfCl_6 and Tl_2ZrCl_6) and

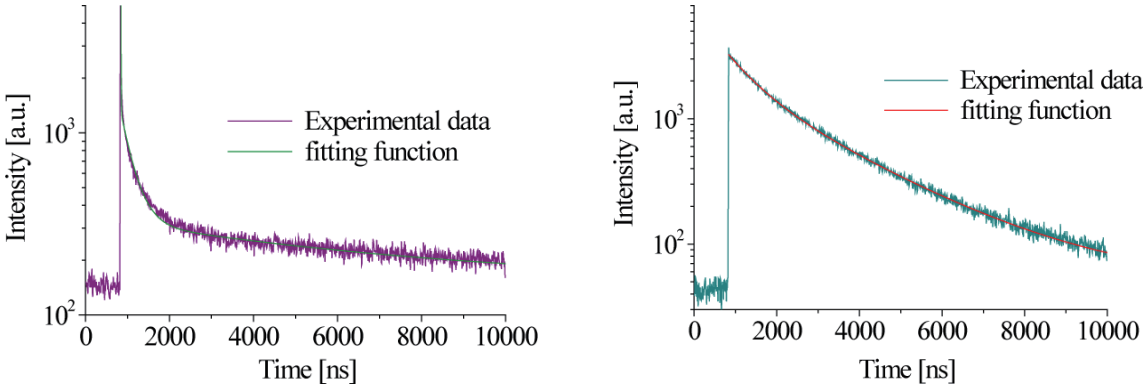

Fig. 5. (Color online) Decay time profiles of pulsed X-ray-excited scintillation for (a) Tl_2HfCl_6 and (b) Tl_2ZrCl_6 crystals.

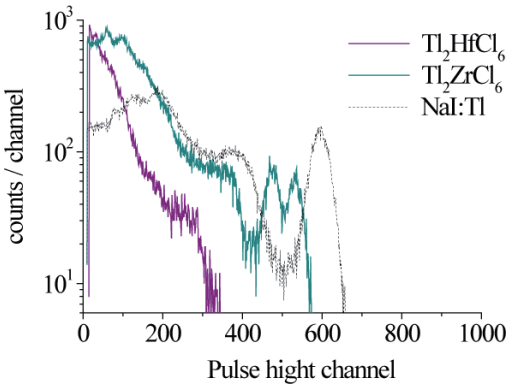

Fig. 6. (Color online) ^{137}Cs-gamma-ray-irradiated scintillation pulse height spectra of Tl_2HfCl_6 (purple line) and Tl_2ZrCl_6 (green line) crystals and a NaI:Tl scintillator spectrum (black dot-line) for comparison.

415 nm (NaI:Tl) were about 28 and 40%, respectively. Thus, the light yields of Tl_2HfCl_6 and Tl_2ZrCl_6 crystals were calculated to be approximately 24200 and 50800 photons/MeV on the basis of a comparison of NaI:Tl. The energy resolutions (FWHMs) of the 662 keV photopeak are approximately 17.7% for Tl_2HfCl_6 and 5.6% for Tl_2ZrCl_6. From the measurements, the Tl_2ZrCl_6 crystal was particularly found to show a high scintillation light yield with good energy resolution, possibly because crystalline quality depends on the purity of starting materials and the crystal growth conditions. The poor energy resolution for Tl_2HfCl_6 is possibly due to low crystalline quality and chemical composition uniformity because of the high vapor pressure of $HfCl_4$ during melt growth.[24] We expect that further improvement of the quality and composition uniformity of Tl_2HfCl_6 can result in a higher energy resolution.

4. Summary

Two new intrinsic crystalline scintillators, Tl_2HfCl_6 and Tl_2ZrCl_6, were reported. Crystal samples of Tl_2HfCl_6 and Tl_2ZrCl_6 were successfully grown by the vertical Bridgman–Stockbarger method. For both Tl_2HfCl_6 and Tl_2ZrCl_6 crystals, the photoluminescence and scintillation spectra showed an emission band peak at 450–470 nm without any internal doping

of an emission center. The scintillation light yields were calculated to be approximately 24200 photons/MeV with the energy resolution of 17.7% at 662 keV for Tl_2HfCl_6 and 50800 photons/MeV with the energy resolution of 5.6% at 662 keV for Tl_2ZrCl_6. For Tl_2HfCl_6, the scintillation decay time value was estimated to be approximately 288 and 6340 ns, while Tl_2ZrCl_6 gave the decay time values of 696 and 2360 ns. Both Tl_2HfCl_6 and Tl_2ZrCl_6 crystals had an emission band peak at 450–470 nm with a high scintillation light yield, which well matched the sensitivity wavelengths of the commercial PMT and Si-based photodiodes. Future efforts toward understanding the origin of these emissions and growing high-quality crystals are expected to further improve the scintillation characteristics. This study indicates that the Tl_2HfCl_6 and Tl_2ZrCl_6 crystalline scintillators can be promising candidates for next-generation X-ray and gamma-ray detectors for various applications.

Acknowledgments

This work was partially supported by the Cooperative Research Project of the Research Institute of Electronics, Shizuoka University.

References

1 C. W. E. van Eijk: Phys. Med. Biol. **47** (2002) R85.
2 E. V. van Loef, C. M. Wilson, N. J. Cherepy, G. Hull, S. A. Payne, W-.S. Choong, W. W. Moses, and K. S. Shah: IEEE Trans. Nucl. Sci., **56** (2009) 869.
3 K. S. Shah, J. Glodo, W. Higgins, E. V. D. van Loef, W. W. Moses, S. E. Derenzo, and M. J. Weber: IEEE Trans. Nucl. Sci. **52** (2005) 3157.
4 A. Burger, E. Rows, M. Groza, K. M. Figueroa, N. J. Cherepy, P. R. Beck, S. Hunter, and S. A. Payne: Appl. Phys. Lett. **107** (2015) 143505.
5 S. Lam, C. Guguschev, A. Burger, M. Hackett, and S. Motakef: J. Cryst. Growth **483** (2018) 121.
6 H. J. Kim, G. Rooh, H. Park, and S. Kim: J. Lumin. **164** (2015) 86.
7 H. J. Kim, G. Rooh, H. Park, and S. Kim: Rad. Meas. **90** (2016) 279.
8 G. Rooh, H. J. Kim, J. Jang, and S. Kim: J. Lumin. **187** (2017) 347.
9 R. Hawrami, E. Ariesanti, H. Wei, J. Finkelstein, J. Glodo, and K. Shah: Cryst. Growth Des. **17** (2017) 3960.
10 K. Watanabe, M. Koshimizu, T. Yanagida, Y. Fujimoto, and K. Asai: Jpn. J. Appl. Phys. **55** (2016) 02BC20.
11 M. Shimizu, M. Koshimizu, Y. Fujimoto, T. Yanagida, S. Ono, and K. Asai: Opt. Mater. **61** (2016) 115.
12 K. Saeki, Y. Wakai, Y. Fujimoto, M. Koshimizu, T. Yanagida, and K. Asai: Jpn. J. Appl. Phys. Rapid Commun. **55** (2016) 110311 .
13 Y. Fujimoto, M. Koshimizu, T. Yanagida, G. Okada, K. Saeki, and K. Asai: Jpn. J. Appl. Phys. Rapid Commun. **55** (2016) 090301.
14 Y. Fujimoto, K. Saeki, T. Yanagida, M. Koshimizu, and K. Asai: Rad. Meas. **106** (2017) 151.
15 K. Saeki, Y. Fujimoto, M. Koshimizu, D. Nakauchi, H. Tanaka, T. Yanagida, and K. Asai: Jpn. J. Appl. Phys. Rapid Commun. **57** (2018) 030310.
16 T. Yanagida, Y. Fujimoto, T. Ito, K. Uchiyama, and K. Mori: Appl. Phys. Exp. **7** (2014) 062401.
17 T. Yanagida, Y. Fujimoto, H. Yagi, and T. Yanagitani: Opt. Mater. **36** (2014) 1044.
18 B. Kang and K. Biswas: J. Phys. Chem. C **120** (2016) 12187.
19 R. Kral, V. Babin, E. Mihokova, M. Buryi, V. V. Laguta, K. Nitsch, and M. Nikl: J. Phys. Chem. C **121** (2017) 12375.
20 M. Koshimizu, K. Saeki, Y. Fujimoto, G. Okada, T. Yanagida, S. Yamashita, and K. Asai: Jpn. J. Appl. Phys. **57** (2018) 032401.
21 K. Saeki, Y. Fujimoto, M. Koshimizu, T. Yanagida, and K. Asai: Appl. Phys. Exp. **9** (2016) 042602.
22 T. Yanagida, Y. Fujimoto, M. Koshimizu, N. Kawano, G. Okada, and N. Kawaguchi: J. Phys. Soc. Jpn. **86** (2017) 094201.
23 H. J. Kim, G. Rooh, H. Park, and S. Kim: J. Lumin. **164** (2015) 86.
24 S. Lam, C. Guguschev, A. Burger, M. Hackett, and S. Motakef: J. Cryst. Growth **483** (2018) 121.